N-Glycosylation plays a role in protein folding of human UGT1A9

N-Glycosylation plays a role in protein folding of human UGT1A9

Miki Nakajima, Toshihisa Koga, Haruko Sakai, Hiroyuki Yamanaka, Ryoichi Fujiwara, and Tsuyoshi Yokoi

Drug Metabolism and Toxicology, Faculty of Pharmaceutical Sciences, Kanazawa University, Kanazawa 920-1192, Japan

To whom all correspondence should be sent:

Miki Nakajima, Ph.D.

Drug Metabolism and Toxicology

Faculty of Pharmaceutical Sciences

Kanazawa University

Kakuma-machi, Kanazawa 920-1192, Japan

Tel / Fax +81-76-234-4407

E-mail: nmiki@kenroku.kanazawa-u.ac.jp

Abstract

UDP-glucuronosyltransferases (UGTs) catalyze the glucuronidation of a variety of xeno/endobiotics. UGTs are type I membrane proteins of the endoplasmic reticulum (ER) with a glycosylated luminal domain. In the present study, we investigated the role of *N*-glycosylation in the function of human UGT1A9. Mutation analysis at the potential *N*-glycosylation sites at residues 71, 292, and 344 (from asparagine to glutamine) revealed that all of them were glycosylated, but the extent of glycosylation and/or size of the glycan differed. In comparison with the wild type, these mutants showed decreased enzyme activities in parallel with the extent of the band shift in Western blot analysis. To evaluate the role of glycosylation in the enzyme activity, we produced unglycosylated UGT1A9 by treating HEK293 cells transiently transfected with expression plasmid with tunicamycin. The unglycosylated UGT1A9 was almost inactive, which was not an indirect effect of ER stress. To the contrary, the deglycosylated UGT1A9, which was produced by the treatment with Endo H under the non-denaturing condition, showed the same enzyme kinetics as the control. These results suggest that the glycosylation that occurs during translation is important for the folding of UGT1A9. The thermal stability analysis of the mutated and deglycosylated UGT1A9 proteins supported the findings. In conclusion, we found that the *N*-glycosylation has an important role in the folding of UGT1A9.

Keywords: UGT1A9, *N*-glycosylation, enzyme activity, protein folding

1. Introduction

Over half of all proteins in nature are glycosylated, and more than three quarters of them contain *N*-linked glycan [1]. *N*-Linked glycosylation occurs at the asparagine (N) residue of the NX(S/T) consensus sequence of a protein, where X is any amino acid except proline. It is estimated that approximately 70-90% of the consensus sequences are glycosylated [2]. *N*-Glycosylation is one of the most common and yet complex forms of post-translational modification. It is intricately involved in various cellular processes including protein folding, protein secretion, intracellular trafficking, stability, binding affinity, enzyme activity, and substrate specificity, enabling fine-tuning of a protein's function [3].

UDP-Glucuronosyltransferases (UGTs) are a superfamily of enzymes that catalyze the glucuronidation of numerous xenobiotic and endobiotic compounds [4]. The reaction results in the formation of hydrophilic glucuronides that are easily excreted into bile or urine. Thus, UGTs are centrally involved in the metabolism and detoxification of drugs, pollutants and toxic substances. Currently, 19 human UGTs have been identified and are classified into two families, UGT1 and UGT2. UGTs are type I endoplasmic reticulum (ER) resident membrane proteins with a single transmembrane domain near the carboxyl-terminus, and most parts including the catalytic domain are located on the luminal side [5,6]. Earlier studies have reported that several UGT isoforms such as human UGT1A6 [7], UGT2B7, UGT2B15, UGT2B17, monkey UGT2B20 [8], rat UGT2B1, and UGT2B2 [9] are *N*-glycosylated. Accumulating evidence suggests that some proteins are dependent on the glycosylation for biological activity, whereas the function of others is not altered by this post-translational modification. As for UGTs, it has been demonstrated that deglycosylation of the purified rabbit UGT1A6, UGT2B13, rat UGT1A6 and UGT2B2 proteins by endoglycosidase H (Endo H) did not decrease their enzyme activities [10]. Mackenzie [9] has reported that rat UGT2B1 and UGT2B2 are *N*-glycosylated and the treatment of COS cells expressing these UGTs with tunicamycin, which inhibits the first step of *N*-glycosylation, i.e., translocation of oligosaccharide core units to peptides, resulted in the production of less active enzymes.

However, the unglycosylated proteins showed similar substrate specificity and protein stability as the native proteins. Barbier et al. [8] have reported that human UGT2B15 and monkey UGT2B20, in which the glycosylation was abolished by the mutation of asparagine residues, showed decreased velocity of glucuronidation, but no changes in the Km values and substrate specificities. Additionally, it has been demonstrated that some other UGT isoforms including human UGT2B4, monkey UGT2B23, and rat UGT2B3 are not glycosylated [8,11]. Thus, the physiological and biological significance of the *N*-glycosylation of UGT proteins remains to be clarified. In this study, we evaluated the role of *N*-glycosylation of human UGT1A, focusing UGT1A9 because it catalyzes the glucuronidation of a variety of drugs, dietary constituents, steroids, and fatty acids [12-14] and there is no report for the glycosylation of this enzyme. We performed a series of studies using Endo H and tunicamycin as well as mutation analysis for recombinant UGT1A9 enzyme. Kinetic analysis, SDS-PAGE analysis under the non-reducing condition, and thermal stability analysis were conducted to elucidate the role of glycosylation of UGT1A9.

2. Materials and Methods

2.1. Materials

O-Glycosidase, tunicamycin, UDP-glucuronic acid (UDPGA), alamethicin 4-methylumbelliferone (4-MU), and 4-MU *O*-glucuronide were purchased from Sigma-Aldrich (St. Louis, MO). Endoglycosidase H (Endo H) was from New England Biolabs (Ipswich, MA). Castanospermin, 1-deoxynojirimycin, thapsigargin, G-418 and propofol were purchased from Wako Pure Chemicals (Osaka, Japan). Rabbit anti-human UGT1A antibodies were obtained from BD Gentest (Woburn, MA). Rabbit anti-human GAPDH antibodies and mouse anti-KDEL antibodies were from Imgenex (San Diego, CA) and Stressgen (Ann Arbor, MI), respectively. IRDye680-labeled goat anti-rabbit secondary antibody and Odyssey Blocking Buffer were from Li-COR Biosciences (Lincoln, NE). Perfect NT Gel M was purchased from DRC (Tokyo, Japan). Taq DNA polymerase was

obtained from Greiner Japan (Tokyo, Japan). Primers were commercially synthesized at Hokkaido System Sciences (Sapporo, Japan). Restriction enzymes were purchased from Takara (Shiga, Japan), Toyobo (Osaka, Japan), Stratagene (La Jolla, CA), and New England Biolabs (Beverly, MA). Lipofectamine 2000 was purchased from Invitrogen (Carlsbad, CA). All other chemicals and solvents were of the highest or analytical grade commercially available.

2.2. Treatment of recombinant UGT1As with Endo H or O-glycosidase

HEK293 cells stably expressing UGT1A1, UGT1A4, UGT1A6, or UGT1A9 were previously established in our laboratory [15]. The cells were grown in Dulbecco's modified Eagle's medium containing 4.5 g/l glucose, 10 mM HEPES, and 10% fetal bovine serum with 5% CO_2 at 37°C. Total cell homogenates were prepared by a method described previously [15]. Briefly, the cells were suspended in Tris-buffered saline [25 mM Tris-HCl buffer (pH 7.4), 138 mM NaCl, and 2.7 mM KCl] and disrupted by freeze-thawing three times. The suspensions were homogenized with a Teflon-glass homogenizer for 10 strokes. The protein concentrations of the homogenates were determined according to Bradford [16]. Then, the homogenates were adjusted to a 2 mg/ml protein concentration with a denaturing buffer in a final concentration of 0.5% SDS and 40 mM DTT, and were denatured at 95°C for 10 min. The denatured proteins (10 μg) were incubated with 250 U of Endo H or 2.5 mU of *O*-glycosidase in 50 mM sodium citrate buffer (pH 5.5) in a final volume of 10 μl at 37°C for 1 h, and were subjected to SDS-PAGE and immunoblotting. For the evaluation of enzyme activity, the recombinant UGT1A9 was treated with Endo H under the non-denaturing condition as follows: the total cell homogenates (10 μg) were incubated with 250 U Endo H in 200 mM Tris-HCl buffer (pH 7.5) in a final volume of 20 μl at 37°C for 1 h.

2.3. SDS-PAGE and immunoblotting

The samples were boiled for 3 min in Laemmli sample buffer containing 2-mercaptoethanol and separated on a 10% SDS-polyacrylamide gel. The separated proteins

were electrotransferred onto PVDF membrane Immobilon-P (Millipore, Billerica, MA). The membrane was washed with phosphate buffered saline (PBS) two times and blocked with Odyssey Blocking Buffer (Li-COR Biosciences, Lincoln, NE) for 1 h. The membranes were incubated with rabbit anti-human UGT1A polyclonal antibody (1:500), rabbit anti-human GAPDH antibodies (1:1000), or mouse anti-KDEL antibodies (1:200) diluted with Odyssey Blocking Buffer containing 0.1% Tween-20 for 1 h. The membrane was washed with PBST (PBS containing 0.1% Tween-20) four times and incubated with IRDye680-labeled goat anti-rabbit or anti-mouse IgG secondary antibody diluted (1:5000) with PBST for 1 h. The densities of the bands were determined using an Odyssey infrared imaging system (Li-COR Biosciences).

2.4. Construction of expression plasmids of UGT1A9 mutants and transient transfection into HEK293 cells

Asparagine residues at the positions 71, 292, and 344 of UGT1A9 were mutated to glutamine using a QuickChange Site-Directed Mutagenesis Kit (Stratagene). The primer sets to construct the expression plasmids of single mutants N71Q, N292Q, and N344Q are shown in Table 1. The expression plasmids of double mutants N71Q/N292Q, N292Q/N344Q, and N71Q/N344Q and a triple mutant N71Q/N292Q/N344Q were constructed by digestion with appropriate restriction enzymes and ligation of the expression plasmids of single mutants. Nucleotide sequences were confirmed by DNA sequence analysis. HEK293 cells (1×10^6 cells) seeded on 6-well plates were transfected with 4 μg of the expression plasmids using Lipofectamine 2000. After 48 h, the total cell homogenates were prepared as described above.

2.5. 4-MU O-glucuronosyltransferase activity

4-MU *O*-glucuronosyltransferase activity was determined as described previously [15]. Briefly, a typical incubation mixture (200 μl of total volume) contained 50 mM Tris-HCl buffer (pH 7.4), 10 mM $MgCl_2$, 2.5 mM UDPGA, 25 μg/ml alamethicin, 0.1 mg/ml cell homogenate, and 50 μM 4-MU. The reaction was initiated by the addition of UDPGA

following a 3-min preincubation at 37°C. After incubation at 37°C for 30 min, the reaction was terminated by the addition of 100 μl of ice-cold methanol. After removal of the protein by centrifugation at 13,000 g for 5 min, a 50-μl portion of the sample was subjected to HPLC. The analytical column was a CAPCEL PAK C18 UG120 (4.6 x 150 mm, 5 μm; Shiseido, Tokyo, Japan), and the mobile phase was 30% methanol/20 mM potassium phosphate buffer (pH 4.5). The eluent was monitored at 320 nm. The quantification of 4-MU *O*-glucuronide was performed by comparing the HPLC peak height to that of the authentic standard.

In kinetic analyses, the 4-MU concentrations varied from 0.5 μM to 50 μM when the UDPGA concentration was fixed at 2.5 mM; the UDPGA concentrations varied from 1 μM to 150 μM when the 4-MU concentration was fixed at 50 μM. Kinetic parameters were estimated from the fitted curve using a computer program (KaleidaGraph, Synergy Software, Reading, PA) designed for non-linear regression analysis. The following equations were applied for Michaelis-Menten kinetics:

$$V = V_{max} \bullet S/ (K_m + S)$$

where V is the velocity of the reaction, S is the substrate concentration, K_m is the Michaelis-Menten constant and V_{max} is the maximum velocity. Data are expressed as the mean ± SD of triplicate determinations.

2.6. Treatment of HEK293 cells expressing wild-type UGT1A9 with glycosylation inhibitors

The HEK293 cells were transiently transfected with 4 μg of the expression plasmid of the wild-type UGT1A9. After 5 h, the cells were treated with tunicamycin (0.025 – 1 μg/ml), castanospermine (100 μg/ml), or 1-deoxynojirimycin (40 μM) for 43 h. As a control experiment to cause ER stress, the cells were treated with thapsigargin (0.5 μM) for 43 h. The total cell homogenates were prepared as described above.

2.7. SDS-PAGE under the non-reducing condition and immunoblotting

SDS-PAGE under the non-reducing condition and immunoblotting were performed as described previously [17] with slight modifications. The total cell homogenate was

solubilized with PBS containing 2% Triton X-100, 0.5% SDS, and 2 mM EDTA, shaking vigorously for 60 min at room temperature, and was centrifuged at 13,000 g for 30 min. To a 24-μl portion of supernatant, 1 μl of 60% glycerol containing 0.2% bromophenol blue was added. The sample (23 μg) was applied to Perfect NT Gel M (5-20% gradient, DRC, Tokyo, Japan). The electrophoresis was carried out at 10 mA for 5 h at 4°C in Tris-glycine electrophoresis buffer (25 mM Tris base, 192 mM glycine, and 0.1% SDS). The separated proteins were transferred to a PVDF membrane Immobilon-P, and the membrane was treated with rabbit anti-human UGT1A polyclonal antibody as described above.

2.8. Examination of thermal instability of UGT1A9

To examine the effects of the deglycosylation on the thermal instability of UGT1A9, the reaction mixtures including the cell homogenate but excluding 4-MU were preincubated at 37, 42, 47, 52 and 57 °C for 15 min in the presence of 2.5 mM UDPGA. The enzyme activities were measured by adding 4-MU in a final concentration of 50 μM at 37°C for 20 min. The residual activity was determined by comparison with the control activity without the preincubation.

2.9. Statistical analyses

Data are expressed as the mean ± SD of three independent determinations. Statistical significance of the kinetic parameters was determined by two-tailed Student's *t* test. A value of $P < 0.05$ was considered statistically significant.

3. Results

3.1. SDS-PAGE analysis of Endo H- or O-glycosidase-treated recombinant human UGT1As

In the SDS-PAGE analysis, human UGT1A1, UGT1A4, UGT1A6, and UGT1A9 stably expressed in HEK293 cells migrated differently (Fig. 1A), although they had quite similar numbers of amino acids (527 to 530 residues). To investigate whether the difference was due to the glycosylation, UGT1As were treated with Endo H and *O*-glycosidase, which cleave *N*-

and *O*-glycosylation sites, respectively. When the UGT1A1, UGT1A4, UGT1A6, and UGT1A9 treated with Endo H were separated, they showed the same migration patterns, which were faster than those of non-treated UGT1As. In contrast, the treatment with *O*-glycosidase did not affect the migration pattern of the original UGT1As. These results suggested that all of UGT1A1, UGT1A4, UGT1A6, and UGT1A9 were *N*-glycosylated. As deduced from the amino acid sequences, UGT1A1 and UGT1A9 have three potential *N*-linked glycosylation sites, NX(S/T) (Fig. 1B). UGT1A4 and UGT1A6 have five and two potential *N*-glycosylation sites, respectively. The differences in the migration of UGT1As on SDS-PAGE seemed to be in parallel with the differences in the number of the potential *N*-glycosylation sites. In the subsequent study, we focused on UGT1A9.

3.2. Effects of substitution of asparagine residues at the potential N-glycosylation sites of UGT1A9 on the migration on SDS-PAGE and the enzyme activity

To investigate the role of the glycosylation on the enzyme activity, three asparagine residues at 71, 292, and 344 of UGT1A9, the potential glycosylation sites, were substituted to glutamine. On the SDS-PAGE analysis, the single mutants N71Q and N344Q showed two bands that migrated faster than those of the wild type (Fig. 2A). The migration of two bands of the single mutants N292Q was slightly faster than those of the wild-type UGT1A9. The double mutants N71Q/N292Q and N292Q/N344Q showed a single band the migration of which was similar to the faster ones observed in the single mutants N71Q and N344Q, respectively. The double mutant N71Q/N344Q showed two bands, of which the band with faster migration seemed to be the same as the band of the triple mutant N71Q/N299Q/N344Q. The migration of the triple mutant was the same as the band of the Endo H-treated wild type. These results indicate that all of the three asparagine residues would be glycosylated, although the extent of glycosylation and/or size of the glycan at residue 292 would be lower than at the other residues.

The 4-MU *O*-glucuronosyltransferase activities by wild-type and mutants UGT1A9 were determined (Fig. 2B). The activities were normalized with the UGT1A9 protein levels

determined by immunoblotting. The kinetics of the activities by the wild-type UGT1A9 was fitted to Michaelis-Menten kinetics. With the varied concentrations of 4-MU and the concentration of UDPGA fixed at 2.5 mM, the Km and Vmax values were 2.7 ± 0.8 μM and 2.33 ± 0.29 nmol/min/unit, respectively (Table 2). With the varied concentrations of UDPGA and the concentration of 4-MU fixed at 50 μM, the Km and Vmax values were 14.1 ± 1.4 μM and 1.23 ± 0.06 nmol/min/unit, respectively. The single mutants N71Q, N292Q, and N344Q showed lower Vmax values than that of the wild type, but no difference was observed in the Km values in comparison with the wild type. The order of intrinsic clearance was N292Q > N344Q > N71Q. The double mutants N71Q/N292Q and N292Q/N344Q showed much lower activities, and the double mutant N71Q/N344Q and the triple mutant N71Q/N292Q/N344Q showed no activity. These results suggest that the substitution of asparagine residues resulted in the production of unglycosylated and inactive protein.

3.3. Effects of treatments with tunicamycin, castanospermine, or 1-deoxynojirimycin on the migration on SDS-PAGE and the enzyme activity of UGT1A9

In the mutation study, we could not exclude the possibility that the loss of enzyme activity may have been due to a change of the protein structure but not due to the lack of glycosylation. To investigate the effect of the glycosylation *per se* on the enzyme activity, we produced unglycosylated protein by treatment with tunicamycin, an inhibitor of oligosaccharyltransferase, which catalyzes the translocation of oligosaccharide core units $(Glc)_3(Man)_9(GlcNAc)_2$ to polypeptides (Fig. 3A). The treatment of the cells with tunicamycin resulted in the production of faster migrating UGT1A9 protein in a dose-dependent manner (Fig. 3B). The mobility of the UGT1A9 protein in the cells treated with 1 μg/ml tunicamycin was the same as that of the Endo H-treated UGT1A9 protein. Thus, we successfully produced unglycosylated UGT1A9 protein. The unglycosylated UGT1A9 protein showed a dose-dependent reduction in enzyme activity associated with the extent of unglycosylation (Fig. 3C). After the glycan core units are transferred to the peptides, the terminus glucoses are trimmed by α-glucosidases I and II in the ER and the Golgi apparatus

(Fig. 3A). To investigate whether the trimming of the terminus glucose may affect the enzyme activity, the cells were treated with castanospermine, an inhibitor of α-glucosidases I and II or 1-deoxynojirimycin, an inhibitor of α-glucosidases II. On the SDS-PAGE, the mobility of UGT1A9 from the cells treated with castanospermine was slightly lower than that of control (Fig. 3B). The effects of the treatment with castanospermine and 1-deoxynojirimycin on the enzyme activity were insignificant (77% and 80% of the control, respectively) (Fig. 3C). These results suggest that the binding of core glycan rather than modification of the terminus would be important to exert the enzyme activity.

It is known that the treatment of cells with tunicamycin causes ER stress by the accumulation of unfolded or misfolded proteins [18,19]. Actually, we observed that the levels of glucose-regulated protein 78 (GRP78) and GRP94 were increased in a dose-dependent manner by treatment with tunicamycin (Fig. 3B). To verify that the decrease of UGT activity would not be due to the secondary effects of ER stress, we determined the UGT activity under the treatment with thapsigargin, an inducer of ER stress inhibiting the Ca^{2+}-ATPase on the ER membrane [20]. The treatment with thapsigargin caused ER stress, demonstrated by the highly increased GRP78 and GRP94, but had little effect on the 4-MU *O*-glucuronosyltransferase activity (81.0% of control) (Fig. 3C). In addition, the treatment with castanospermine or 1-deoxynojirimycin also caused ER stress, but their effects on UGT1A9 activity were insignificant. These results suggest that the dramatic decrease of UGT1A9 activity by tunicamycin treatment would be due to the inhibition of glycosylation during the translation.

3.4. Effects of deglycosylation on the enzyme activity of UGT1A9

Next, we investigated whether the digestion of glycan from the mature UGT1A9 protein might affect the enzyme activity. We measured the 4-MU glucuronosyltransferase activity of the wild-type UGT1A9 that was treated with Endo H under the non-denaturing condition. We first confirmed that UGT1A9 was completely deglycosylated by Endo H (Fig. 4A). The kinetics of 4-MU glucuronosyltransferase activity by deglycosylated UGT1A9 was

similar to that by the non-treated UGT1A9 (Fig. 4B). These results suggest that the glycan per se would not be a determinant of the enzyme kinetics.

3.5. Role of N-glycosylation on the protein folding of UGT1A9

It was surmised that the decreases of the enzyme activity of mutants UGT1A9 as well as the unglycosylated UGT1A9 produced by tunicamycin treatment might result from changes in the protein folding of UGT1A9. To investigate whether the inhibition of *N*-glycosylation affects the higher structure of UGT1A9 protein, we performed SDS-PAGE under the non-reduced condition analysis. As shown in Fig. 5A, in control, two bands were observed at about 53 kDa and 110 kDa, corresponding to a monomer and dimer, respectively, as previously reported [17]. The treatment with castanospermine or 1-deoxynojirimycin did not affect the higher structure of UGT1A9. Unexpectedly, no band was observed with the total cell homogenates from tunicamycin (1 μg/ml)-treated cells, though a clear band was observed in the SDS-PAGE analysis. This may imply that the epitope of UGT1A9 toward the anti-UGT1As antibody might be sterically distorted. In other words, the folding of UGT1A9 might be changed by the inhibition of *N*-glycosylation. To confirm this assumption, we also performed the SDS-PAGE under the non-reduced condition analysis for a series of mutant UGT1A9 proteins (Fig. 5B). Interestingly, the single mutants N71Q and N344Q showed two bands corresponding to a monomer and dimer that were weaker than those of the wild type, although the single mutant N292Q did not show a prominent difference in comparison with the wild type. Three double mutants barely showed the two monomer and dimer bands. Finally, in triple mutants, no clear band was observed, supporting the hypothesis that unglycosylated protein would have aberrant protein folding. In contrast, Endo H-treated UGT1A9 clearly showed the two bands indicating that the deglycosylation from the correctly folded protein did not affect the higher structure of UGT1A9. These results suggest that impeding *N*-glycosylation would cause drastic changes in the folding of UGT1A9.

3.6. Thermally stable characteristics of UGT1A9: asparagine-substituted mutants UGT1A9

and Endo H-treated wild-type UGT1A9

In our previous study [15], we demonstrated that UGT1A9, among human UGT1A isoforms, is uniquely tolerable to heat treatment. The thermal stability of proteins largely depends on their three-dimensional structures. To investigate the role of the *N*-glycosylation on the protein folding of UGT1A9, we determined the thermal stability of single mutants of UGT1A9 or Endo H-treated wild-type UGT1A9. Double and triple mutants and the tunicamycin-treated wild-type UGT1A9 were not used, since their enzyme activities were low. The 4-MU *O*-glucuronosyltransferase activity by the wild-type UGT1A9 was almost completely retained by heat treatment up to 52°C (Fig. 5), showing thermal stability consistent with our previous study [15]. The activity was decreased by 80% of control by heat treatment at 57°C. The single mutants N71Q, N292Q, and N344Q were also stable in response to the heat treatment up to 52°C, but treatment at 57°C decreased their activities (39%, 52%, and 57% of control, respectively), which were significantly lower than those of the wild type. In contrast, the Endo H-treated UGT1A9 showed thermal stability similar to that of the non-treated UGT1A9. These results suggest that *N*-glycosylation would be important for the protein folding of UGT1A9.

4. Discussion

In the present study, we evaluated the role of *N*-glycosylation in human UGT1As and found that all of the UGT1A1, 1A4, 1A6, and 1A9 were *N*-glycosylated. It was not a specific phenomenon for the recombinant proteins, because we observed the Endo H-dependent shift of bands when human liver microsomes were applied for the SDS-PAGE analysis using isoform-specific antibodies against human UGT1A1, UGT1A6 (BD Gentest), and UGT1A9 [21] (data not shown). The numbers of the potential *N*-glycosylation sites of UGT1A1, 1A4, 1A6, and 1A9 are 3, 5, 2, and 3, respectively (Fig. 1B), and seem to be in parallel with the molecular sizes of these glycoproteins (Fig. 1A). By the mutation analysis, we found that the three potential glycosylation sites at position 71, 292, and 344 in UGT1A9 were all glycosylated, although the extent of glycosylation and/or size of the glycan at position 292

would be low. Previously, Ouzzine et al. [7], using mutation analysis of recombinant enzymes expressed in yeast, reported that human UGT1A6 is glycosylated at position 345, but not at 293. They concluded from the results of the SDS-PAGE and immunoblot analysis that there was no difference between the mobility of the mutant N293G and the wild-type UGT1A6. Consistent with their finding, as shown in Fig. 2A, the difference in the mobility between the mutant N292Q and wild-type UGT1A9 was not large. However, analysis with the combination mutants at three sites revealed that N292 would be *N*-glycosylated. The enzyme kinetic analysis also supported this (Fig. 2 and Table 2). Thus, it is conceivable that human UGT1As are commonly *N*-glycosylated at the sites corresponding to N292 and N344 of UGT1A9, which are encoded from common exons 2 and 5, although the extent of glycosylation and/or size of the glycan are different. The mutation of these asparagine residues significantly decreased the Vmax values, but not the Km values (Table 2), consistent with a previous study of human UGT2B15 and monkey UGT2B20 [8]. To investigate whether the decreased velocity was due to the abolished glycosylation, not by the change in primary structure, we further studied the enzyme activity of unglycosylated and deglycosylated UGT1A9 proteins.

The unglycosylated UGT1A9 protein produced by the treatment with tunicamycin was enzymatically inactive. In addition, the SDS-PAGE under the non-reduced condition analysis revealed that it had aberrant folding. Therefore, the decreased enzyme activity would result from the misfolding owing to the abolished glycosylation. The thermal stability assays supported the importance of glycosylation in the folding of UGT protein. Once UGTs are correctly folded in the presence of glycan, they are enzymatically active, because the deglycosylation of UGT1A9 by Endo H did not affect the enzyme activity. These results also suggest that the *N*-glycosylation is important for the folding of UGT proteins. The C-terminal half including two *N*-glycosylation sites is common to UGT1A isoforms. Therefore, it would be reasonable to assume that the importance of *N*-glycosylation is common to UGT1As. Supporting it, we found that unglycosylated UGT1A1 protein produced by the treatment with tunicamycin was enzymatically inactive, whereas the kinetics of 4-MU

glucuronosyltransferase activity by UGT1A6 was also not affected by deglycosylation with Endo H (data not shown). However, it should be pointed out that some UGT2B isoforms are not glycosylated. Barbier et al. [8] reported that human UGT2B4, monkey UGT2B18 and UGT2B23 are not *N*-glycosylated in spite of the presence of the potential *N*-glycosylation sites. Additionally, there is no potential *N*-glycosylation site for rat UGT2B3 [9] and UGT2B6 [10]. Although the precise mechanisms of the folding of UGTs are not known, glycosylated UGTs and non-glycosylated UGTs may be differently regulated. It would be of interest to determine whether such a difference affects the higher structures, stabilities, and membrane-traffic of UGTs in the future.

In the present study, we determined 4-MU glucuronosyltransferase activity to evaluate the effects of *N*-glycosylation on the enzyme activity of UGT1A9. Additionally, to investigate whether the effects of *N*-glycosylation might be different depending on substrates, we also determined propofol *O*-glucuronosyltransferase activities. The unglycosylated UGT1A9 produced by the treatment with tunicamycin was inactive for propofol *O*-glucuronidation, and the effects of the mutations of each *N*-glycosylation site on the kinetics of propofol glucuronidation were similar with those observed in the 4-MU glucuronidation (data not shown). In addition, the kinetics of the deglycosylated UGT1A9 by Endo H was completely fitted with that by the non-treated UGT1A9 (data not shown). Thus, it is unlikely that the effects of *N*-glycosylation would be depending on substrates.

In conclusion, we found that human UGT1A9 was *N*-glycosylated, and impeding *N*-glycosylation resulted in the loss of function. This study clearly demonstrated that the *N*-glycosylation plays an important role in the protein folding of UGT1A9.

Acknowledgement

We acknowledge Mr. Brent Bell for reviewing the manuscript.

References

[1] Apweiller R, Hermjakob H, Sharon N. Newer aspects of glucuronidetion. Biochim Biophys Acta 1999; 1473: 4-8.

[2] Gravel Y, von Heijne G. Sequence differences between glycosylated and non-glycosylated Asn-X-Thr/Ser acceptor sites: implications for protein engineering. Protein Eng 1990; 3: 433-42.

[3] Skropeta D. The effect of individual N-glycans on enzyme activity. Bioorg Med Chem 2009; 17: 2645-53.

[4] Tukey RH, Strassburg CP. Human UDP-glucuronosyltransferases: metabolism, expression, and disease. Annu Rev Pharmacol Toxicol 2000; 40: 581-616.

[5] Dutton GJ, Burchell B. Newer aspects of glucuronidation. Prog Drug Metab 1977; 2: 1-70.

[6] Dutton GJ. Acceptor substrates of UDP-glucuronosyltransferase and their assay, in Glucuronidation of Drugs and Other Compounds (Dutton GJ ed). Boca Raton, FL: CRC Press, 1980, p 69-78.

[7] Ouzzine M, Barré L, Netter P, Magdalou J, Fournel-Gigleux S. Role of the carboxyl terminal stop transfer sequence of UGT1A6 membrane protein in ER targeting and translocation of upstream lumenal domain. FEBS Lett 2006; 580: 1953-1958.

[8] Barbier O, Girard C, Breton R, Bélanger A, Hum DW. N-glycosylation and residue 96 are involved in the functional properties of UDP-glucuronosyltransferase enzymes. Biochemistry 2000; 39: 11540-52.

[9] Mackenzie PI. The effect of N-linked glycosylation on the substrate preferences of UDP glucuronosyltransferases. Biochem Biophys Res Commun 1990; 166: 1293-9.

[10] Green MD, Tephly N-glycosylation of purified rat and rabbit hepatic UDP-glucuronosyltransferases. Arch Biochem Biophys 1989; 273: 72-8.

[11] Mackenzie PI. Expression of chimeric cDNAs in cell culture defines a region of UDP glucuronosyltransferase involved in substrate selection. J Biol Chem 1990; 265: 3432-5.

[12] Ritter JK. Roles of glucuronidation and UDP-glucuronosyltransferases in xenobiotic bioactivation reactions. Chem Biol Interact. 2000; 129: 171-93.

[13] Turgeon D, Chouinard S, Belanger P, Picard S, Labbe JF, Borgeat P et al. Glucuronidation of arachidonic and linoleic acid metabolites by human UDP-glucuronosyltransferases. J Lipid Res. 2003; 44: 1182-91.

[14] Chen Y, Xie S, Chen S, Zeng S. Glucuronidation of flavonoids by recombinant UGT1A3 and UGT1A9. Biochem Pharmacol. 2008; 76: 416-25.

[15] Fujiwara R, Nakajima M, Yamanaka H, Nakamura A, Katoh M, Ikushiro S et al. Effects of coexpression of UGT1A9 on enzymatic activities of human UGT1A isoforms. Drug Metab Dispos 2007; 35: 747-57.

[16] Bradford MM. Rapid and sensitive method for the quantitation of microgram quantities of protein utilizing the principle of protein-dye binding. Anal Biochem 1976; 72: 248-54.

[17] Fujiwara R, Nakajima M, Yamanaka H, Katoh M, Yokoi T. Interactions between human UGT1A1, UGT1A4, and UGT1A6 affect their enzymatic activities. Drug Metab Dispos 2007; 35: 1781-7.

[18] Han C, Nam MK, Park HJ, Seong YM, Kang S, Rhim H. Tunicamycin-induced ER stress upregulates the expression of mitochondrial HtrA2 and promotes apoptosis through the cytosolic release of HtrA2. J Microbiol Biotechnol 2008; 18: 1197-202.

[19] Görlach A, Klappa P, Kietzmann T. The endoplasmic reticulum: folding, calcium homeostasis, signaling, and redox control. Antioxid Redox Signal 2006; 8: 1391-418.

[20] Thastrup O, Cullen PJ, Drøbak BK, Hanley MR, Dawson AP. Thapsigargin, a tumor promoter, discharges intracellular Ca^{2+} stores by specific inhibition of the endoplasmic reticulum Ca^{2+}-ATPase. Proc Natl Acad Sci USA 1990; 87: 2466-70.

[21] Ikushiro S, Emi Y, Kato Y, Yamada S, Sakaki T. Monospecific antipeptide antibodies against human hepatic UDP-glucuronosyltransferase 1A subfamily (UGT1A) isoforms. Drug Metab Pharmacokinet 2006; 21: 70-4.

Figure legends

Fig. 1. SDS-PAGE and immunoblotting of Endo H- or *O*-glycosidase-treated human UGT1A proteins and potential *N*-glycosylation site. (A) Total cell homogenates from HEK293 cells stably expressing UGT1A1, UGT1A4, UGT1A6, or UGT1A9 were treated with Endo H or *O*-glycosidase as described in Materials and Methods. The samples (10 μg) were subjected to 10% SDS-PAGE and transferred to a PVDF membrane. The membrane was probed with an anti-human UGT1A antibody. (B) Schematic representation of UGT1A proteins and potential *N*-glycosylation sites. UGT1As are generated by alternative splicing of unique exon 1 to common exons 2-5, resulting in isoforms with an identical C-terminal half of protein and a unique N-terminal half.

Fig. 2. Molecular size and enzyme activity of UGT1A9 mutants. The expression plasmids of wild-type and mutants UGT1A9 were transiently transfected into the HEK293 cells. (A) Total cell homogenates (10 μg) were separated by 10% SDS-PAGE. Endo H-treated cell homogenates (10 μg) expressing wild-type UGT1A9 was also separated to show the migration of non-glycosylated UGT1A9. The band density of the wild-type UGT1A9 was defined as 1 unit per 10 μg of protein. Values were the mean ± SD of three independent determinations. GAPDH levels were examined as a loading control. (B) Kinetic analyses of 4-MU *O*-glucuronosyltransferase activities were performed. Total cell homogenates were incubated with 0.5 to 50 μM 4-MU and UDPGA fixed at 2.5 mM (left panel), or with 1 - 150 μM UDPGA and 4-MU fixed at 50 μM (right panel). Data are the mean ± SD of triplicate determinations.

Fig. 3. Effects of the inhibitors of glycosylation or glycosidase on UGT1A9. (A) Schematic representation of biosynthesis of *N*-glycosylated protein in ER. Tunicamycin inhibits the first step of N-glycosylation, translocation of oligosaccharide core units to peptides. Castanospermine inhibits α-glucosidases I and II and 1-deoxynojirimycin inhibits

α-glucosidase II (B) HEK293 cells were transiently transfected with the expression plasmid of wild-type UGT1A9. After 5 h, the cells were treated with tunicamycin (0.025 to 1 μg/ml), an inhibitor of glycosylation, castanospermine (100 μg/ml) or 1-deoxynojirimycin (40 μM), inhibitors of glycosidase, for 43 h. To induce ER stress, the cells were treated with thapsigargin (0.5 μM) for 24 h. SDS-PAGE and immunoblotting using anti-human UGT1A antibody were performed with 10 μg total cell homogenates. Endo H-treated cell homogenate expressing wild-type UGT1A9 was applied to show the migration of non-glycosylated UGT1A9. The band density of the control UGT1A9 was defined as 1 unit per 10 μg of protein. Values were the mean ± SD of three independent determinations. Immunoblotting using anti-KDEL antibody was performed with 40 μg total cell homogenates to determine the levels of GRP94 and GRP78. The band density of the non-treated cells (control) was defined as 1. GAPDH levels were examined as a loading control. (C) 4-MU *O*-glucuronosyltransferase activities were determined with 50 μM 4-MU and 2.5 mM UDPGA at 37°C for 20 min. Data are the mean ± SD of triplicate determinations. $^{**}P < 0.01$ compared with control.

Fig. 4. Effects of deglycosylation on the enzyme activity of UGT1A9. The total cell homogenates (10 μg) prepared from the HEK293 cells transiently expressing UGT1A9 were treated with 250 U Endo H under the non-denaturing condition (200 mM Tris-HCl buffer, pH 7.5) at 37°C for 1 h. (A) SDS-PAGE and immunoblotting were performed. (B) Kinetic analyses of 4-MU *O*-glucuronosyltransferase activities were performed with 1 to 50 μM 4-MU and UDPGA fixed at 2.5 mM (left panel) or with 2.5 to 150 μM UDPGA and 4-MU fixed at 50 μM (right panel).

Fig. 5. SDS-PAGE under the non-reduced condition and immunoblot analysis. Total cell homogenates from (A) tunicamycin (1 μg/mL)-, castanospermine (100 μg/ml)- or 1-deoxynojirimycin (40 μM)-treated HEK293 cells expressing wild-type UGT1A9, and (B) the HEK293 cells expressing mutants UGT1A9 were separated on Perfect NT Gel M (5-20%

gradient). (C) Endo H-treated homogenates from the HEK293 cells expressing wild-type UGT1A9 were also separated. Immunoblotting was performed as described in Materials and Methods.

Fig. 6. Thermal instability of wild-type and mutants UGT1A9 (A) as well as Endo H-treated UGT1A9 (B). The reaction mixtures including the cell homogenate but excluding 4-MU were preincubated at 37, 42, 47, 52 and 57 °C for 15 min in the presence of 2.5 mM UDPGA. The enzyme activities were measured by adding 4-MU in a final concentration of 50 μM at 37°C for 20 min. The residual activity was determined by comparison with the control activity without the preincubation. Data are the mean ± SD of triplicate determinations. Control activities were as follows: (A) wild-type, 3.09 ± 0.11 nmol/min/unit; N71Q, 0.23 ± 0.01 nmol/min/unit; N292Q, 1.69 ± 0.06 nmol/min/unit; N344Q, 0.40 ± 0.02 nmol/min/unit (B) non-treated, 2.53 ± 0.14 nmol/min/unit; Endo H-treated, 2.48 ± 0.06 nmol/min/unit.

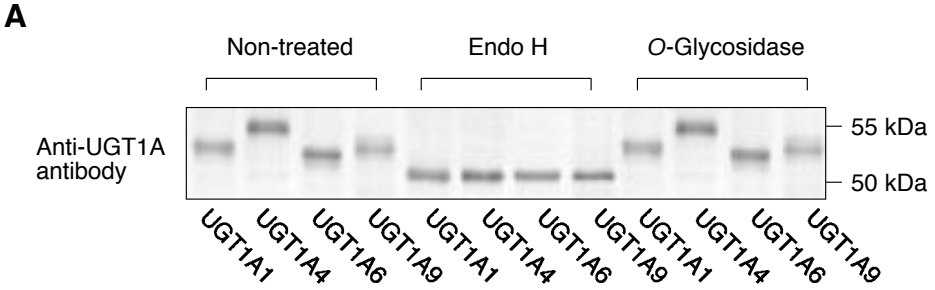
A
Non-treated
Endo H
O-Glycosidase
Anti-UGT1A antibody
55 kDa
50 kDa
UGT1A1
UGT1A4
UGT1A6
UGT1A9
UGT1A1
UGT1A4
UGT1A6
UGT1A9
UGT1A1
UGT1A4
UGT1A6
UGT1A9

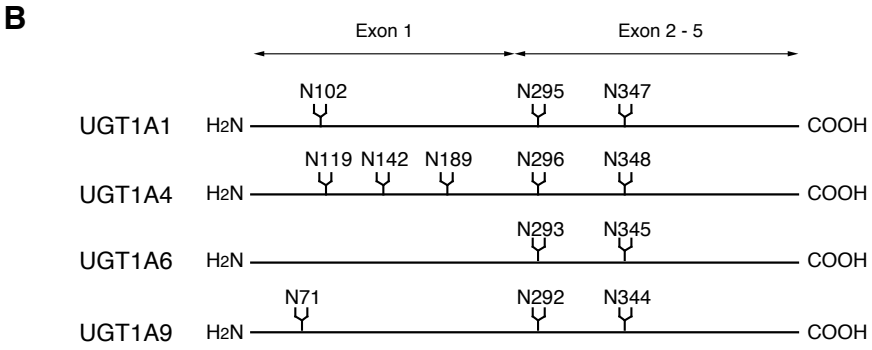
B
Exon 1
Exon 2 - 5
UGT1A1
H2N
COOH
N102
N295
N347
UGT1A4
H2N
COOH
N119
N142
N189
N296
N348
UGT1A6
H2N
COOH
N293
N345
UGT1A9
H2N
COOH
N71
N292
N344

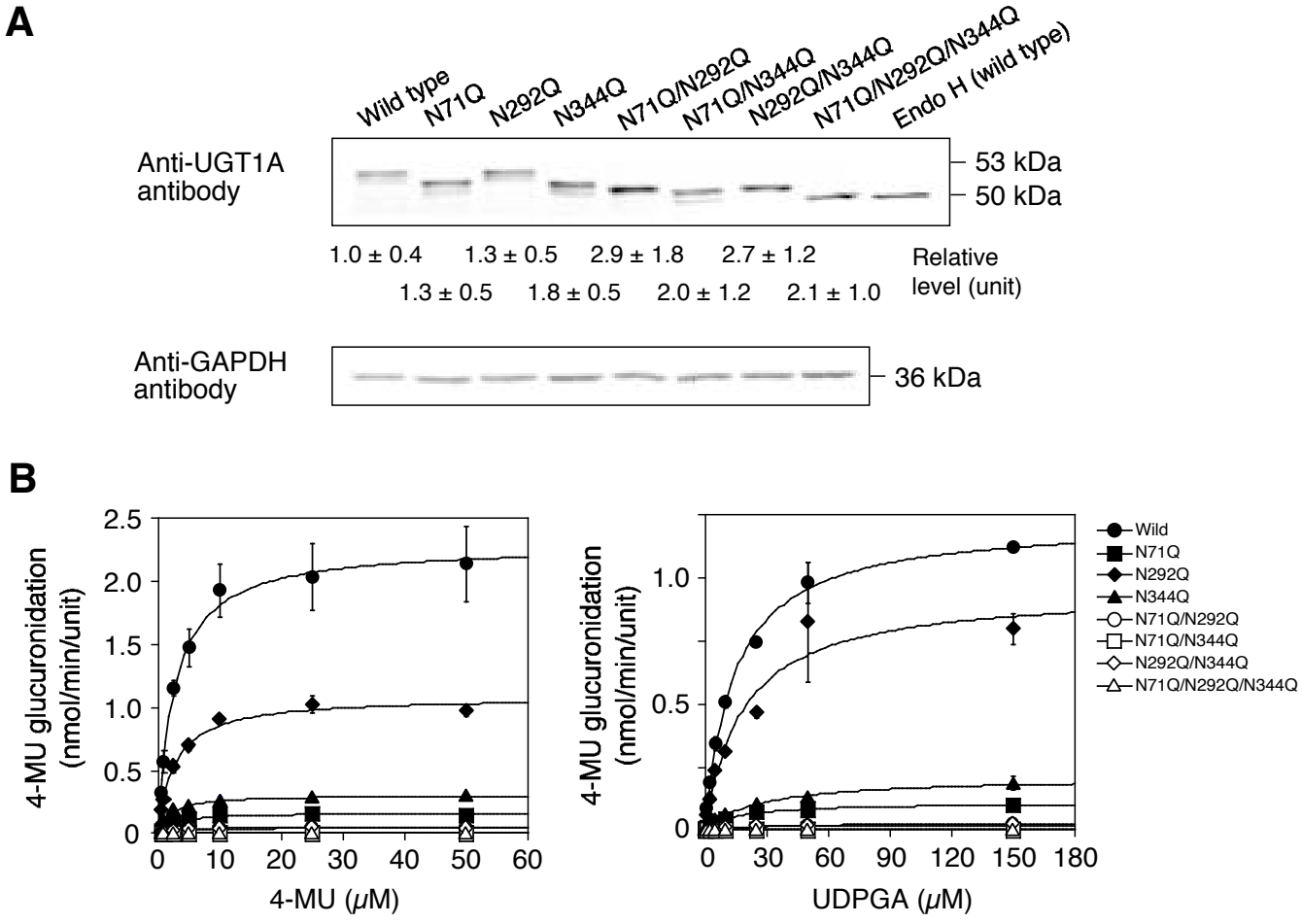
A
Wild type
N71Q
N292Q
N344Q
N71Q/N292Q
N71Q/N344Q
N292Q/N344Q
N71Q/N292Q/N344Q
Endo H (wild type)
Anti-UGT1A antibody
53 kDa
50 kDa
1.0 ± 0.4
1.3 ± 0.5
2.9 ± 1.8
2.7 ± 1.2
1.3 ± 0.5
1.8 ± 0.5
2.0 ± 1.2
2.1 ± 1.0
Relative level (unit)
Anti-GAPDH antibody
36 kDa
B
4-MU glucuronidation (nmol/min/unit)
4-MU (μM)
UDPGA (μM)
Wild
N71Q
N292Q
N344Q
N71Q/N292Q
N71Q/N344Q
N292Q/N344Q
N71Q/N292Q/N344Q

Fig.3

A

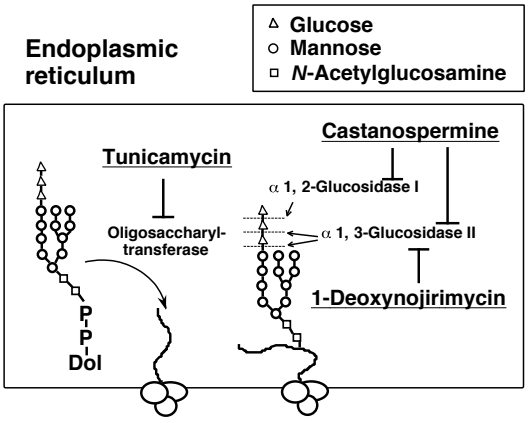
Endoplasmic reticulum
Glucose
Mannose
N-Acetylglucosamine
Castanospermine
Tunicamycin
α 1, 2-Glucosidase I
α 1, 3-Glucosidase II
Oligosaccharyl-transferase
1-Deoxynojirimycin
P-P-Dol

B

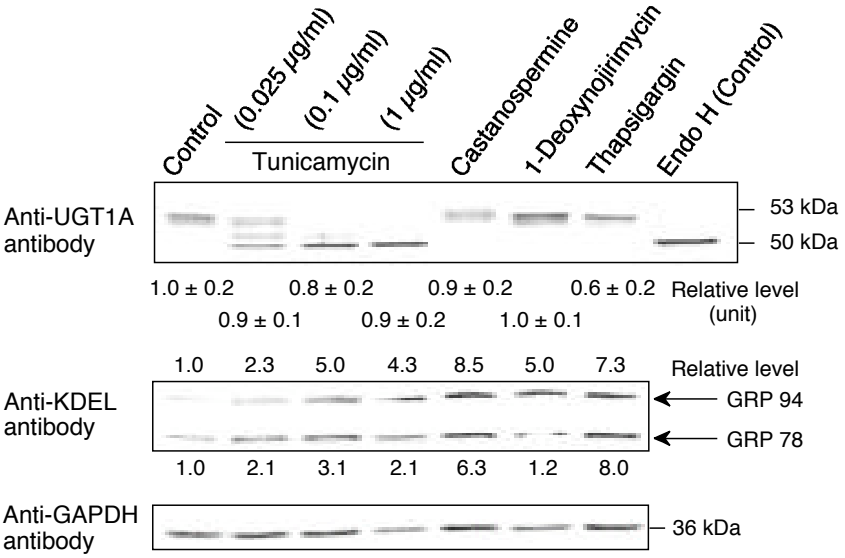
Control
(0.025 μg/ml)
(0.1 μg/ml)
(1 μg/ml)
Tunicamycin
Castanospermine
1-Deoxynojirimycin
Thapsigargin
Endo H (Control)
Anti-UGT1A antibody
53 kDa
50 kDa
1.0 ± 0.2
0.8 ± 0.2
0.9 ± 0.2
0.6 ± 0.2
0.9 ± 0.1
0.9 ± 0.2
1.0 ± 0.1
Relative level (unit)
1.0 2.3 5.0 4.3 8.5 5.0 7.3
Relative level
Anti-KDEL antibody
GRP 94
GRP 78
1.0 2.1 3.1 2.1 6.3 1.2 8.0
Anti-GAPDH antibody
36 kDa

C

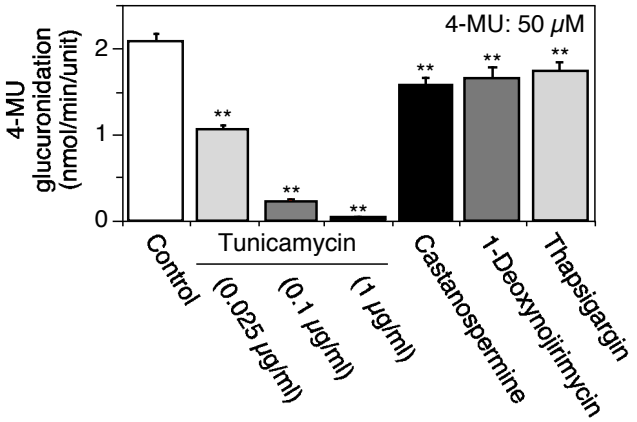
4-MU: 50 μM
4-MU glucuronidation (nmol/min/unit)
2
1
0
**
Control
(0.025 μg/ml)
(0.1 μg/ml)
(1 μg/ml)
Tunicamycin
Castanospermine
1-Deoxynojirimycin
Thapsigargin

A

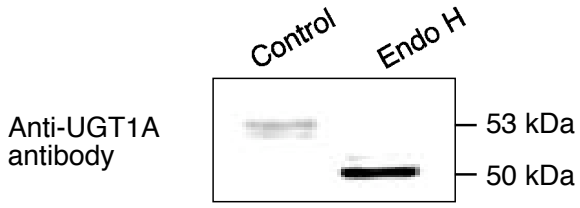
Control
Endo H
Anti-UGT1A antibody
53 kDa
50 kDa

B

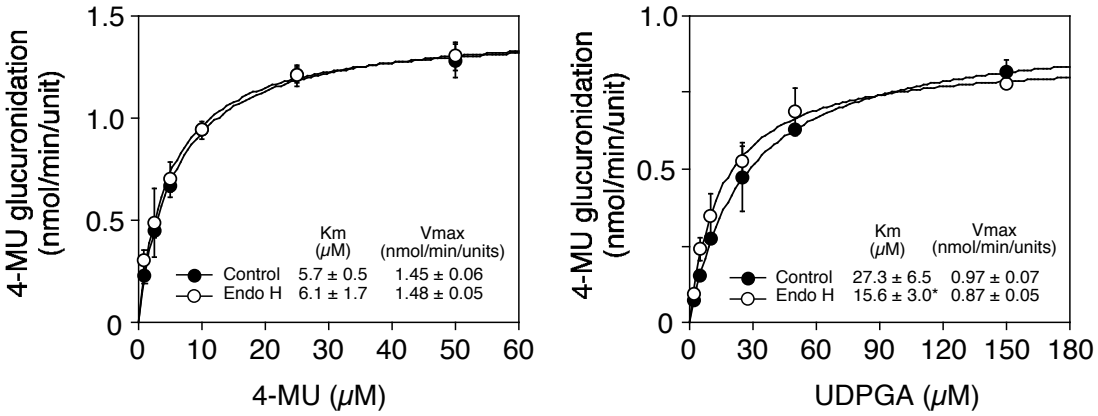
4-MU glucuronidation (nmol/min/unit)
1.5
1.0
0.5
0
0 10 20 30 40 50 60
4-MU (μM)
Km (μM)
Vmax (nmol/min/units)
Control 5.7 ± 0.5 1.45 ± 0.06
Endo H 6.1 ± 1.7 1.48 ± 0.05
4-MU glucuronidation (nmol/min/unit)
1.0
0.5
0
0 30 60 90 120 150 180
UDPGA (μM)
Km (μM)
Vmax (nmol/min/units)
Control 27.3 ± 6.5 0.97 ± 0.07
Endo H 15.6 ± 3.0* 0.87 ± 0.05

Fig. 5

A

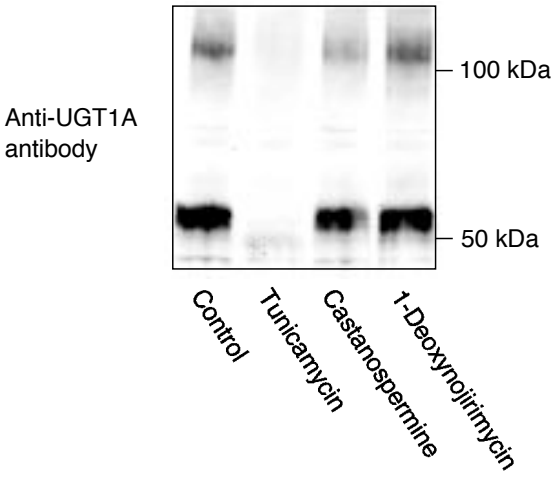
Anti-UGT1A
antibody
100 kDa
50 kDa
Control
Tunicamycin
Castanospermine
1-Deoxynojirimycin

B

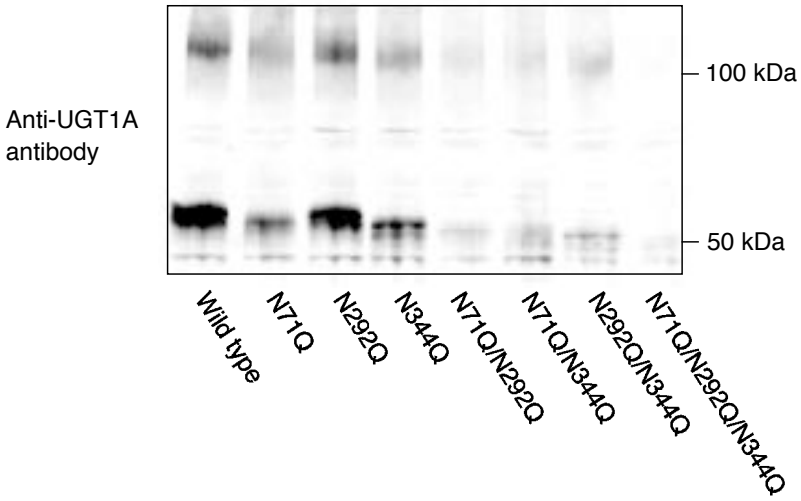
Anti-UGT1A
antibody
100 kDa
50 kDa
Wild type
N71Q
N292Q
N344Q
N71Q/N292Q
N71Q/N344Q
N292Q/N344Q
N71Q/N292Q/N344Q

C

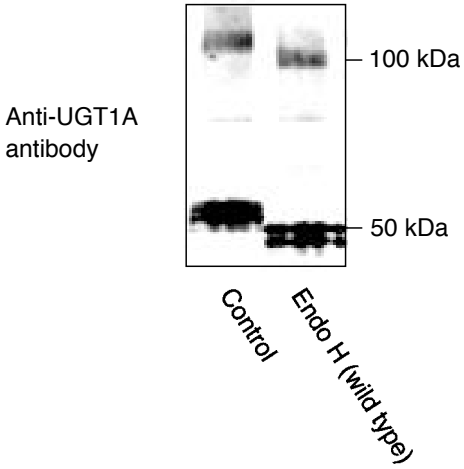
Anti-UGT1A
antibody
100 kDa
50 kDa
Control
Endo H (wild type)

Fig. 6

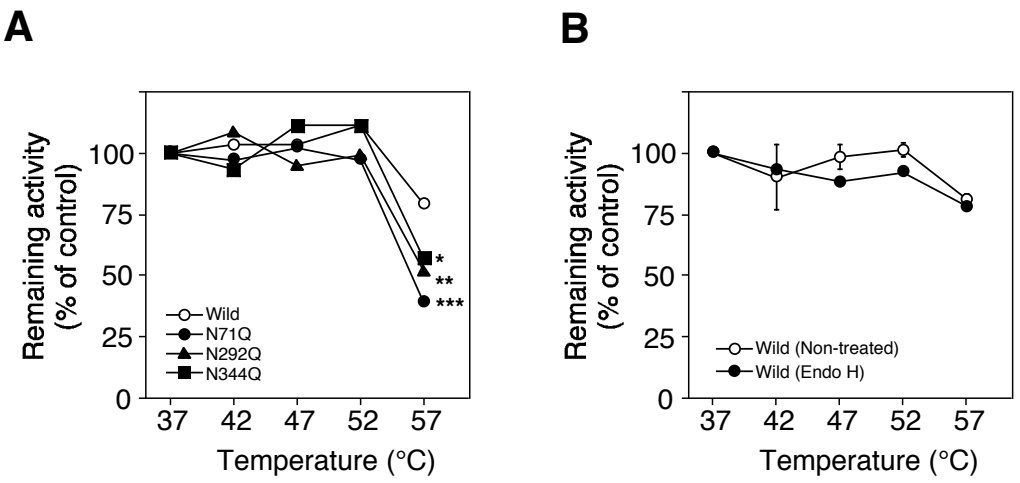
A
Remaining activity (% of control)
100
75
50
25
0
37
42
47
52
57
Temperature (°C)
Wild
N71Q
N292Q
N344Q
*
**
***
B
Remaining activity (% of control)
100
75
50
25
0
37
42
47
52
57
Temperature (°C)
Wild (Non-treated)
Wild (Endo H)

Table 1. Primers used for site-direct mutagenesis of UGT1A9.

Primers	Sequences
N71Q-S	5’-CAACTGGGAAGATCACTGCAGTGCACAGTGAAGACTTATTC-3’
N71Q-AS	5’-GAATAAGTCTTCACTGTGCACTGCAGTGATCTTCCCAGTTG-3’
N292Q-S	5’-GGAATTTGAAGCCTACATTCAGGCTTCTGGAGAACATGGAATTGTGG-3’
N292Q-AS	5’-CCACAATTCCATGTTCTCCAGAAGCCTGAATGTAGGCTTCAAATTCC-3’
N344Q-S	5’-CCGACCATCGAATCTTGCGCAGAACACGATACTTGTTAAG-3’
N344Q-AS	5’-CTTAACAAGTATCGTGTTCTGCGCAAGATTCGATGGTCGG-3’

Table 2. Kinetic parameters for 4-MU *O*-glucuronidation by wild-type and mutants UGT1A9 expressed in HEK293 cells.

Wild/Mutants	Km	Vmax	Vmax/Km
Varied concentration of 4-MU	(μM)	(nmol/min/unit)	(μL/min/unit)
Wild	2.7 ± 0.8	2.33 ± 0.29	886 ± 142
N71Q	2.6 ± 0.1	0.17 ± 0.01**	66 ± 5**
N292Q	2.7 ± 0.2	1.09 ± 0.03**	413 ± 33**
N344Q	1.9 ± 0.4	0.31 ± 0.01**	164 ± 29**
N71Q/N292Q	3.6 ± 0.4	0.05 ± 0.00**	15 ± 1**
N71Q/N344Q	ND	ND	ND
N292Q/N344Q	2.6 ± 0.4	0.05 ± 0.00**	18 ± 3**
N71Q/N292Q/N344Q	ND	ND	ND
Varied concentration of UDPGA	(μM)	(nmol/min/unit)	(μL/min/unit)
Wild	14.1 ± 1.4	1.23 ± 0.06	87 ± 5
N71Q	16.5 ± 5.6	0.11 ± 0.00**	7 ± 2**
N292Q	19.3 ± 3.9	0.97 ± 0.04**	52 ± 11*
N344Q	27.3 ± 8.6	0.22 ± 0.04**	8 ± 1**
N71Q/N292Q	20.2 ± 11.9	0.02 ± 0.00**	1 ± 1**
N71Q/N344Q	ND	ND	ND
N292Q/N344Q	25.1 ± 2.9**	0.03 ± 0.00**	1 ± 0**
N71Q/N292Q/N344Q	ND	ND	ND

Data are the mean ± SD. $^{**}P < 0.01$, $^{*}P < 0.05$ compared with control value.